Astron. Astrophys. 358, 1142–1150 (2000)

ASTRONOMY
AND
ASTROPHYSICS

Accretion and galactic dynamos

D. Moss[1], **A. Shukurov**[2], **and D. Sokoloff**[2,3]

[1] Department of Mathematics, University of Manchester, Manchester M13 9PL, UK
[2] Department of Mathematics, University of Newcastle, Newcastle on Tyne NE1 7RU, UK
[3] Physics Department, Moscow University, Moscow 19899, Russia

Received 5 January 2000 / Accepted 26 April 2000

Abstract. We show that radial flows (directed either inward or outward) suppress mean-field dynamo action in a thin disc. Under conditions typical of spiral galaxies, the reduction in the growth rate of the large-scale magnetic field can reach 25–30%. The dynamo-generated galactic magnetic fields themselves can drive radial flows at a rate of order $0.1\,M_\odot\,\mathrm{yr}^{-1}$. These radial flows can contribute to the saturation of the dynamo action together with other nonlinear effects. We also present arguments, and an illustrative computation, to support the view that in the inner regions of barred galaxies the magnetically driven mass accretion rate may be substantially larger than the above estimate due to deviations of magnetic field from axial symmetry. The magnetically driven inflow rate in barred galaxies can reach about $3\,M_\odot\,\mathrm{yr}^{-1}$.

Key words: accretion, accretion disks – magnetic fields – ISM: magnetic fields – galaxies: magnetic fields

1. Introduction

Radial inflow is a generic feature of astrophysical discs, both in spiral galaxies and in the accretion discs around young stars and in active galactic nuclei. Accretion arises from the angular momentum transport by viscous and magnetic stresses, winds and from nonaxisymmetric gravitational torques, e.g. from galactic density waves and/or bars.

The effects of the radial inflow on the regular galactic magnetic field can be significant. Ruzmaikin (1976) (see also Ruzmaikin et al. 1988, Sect. VI.10) argued that the inflow driven by energy dissipation in spiral shocks can lead to an enhancement of the galactic magnetic field due to the compression term $\boldsymbol{B}(\nabla\cdot\boldsymbol{v})$ in the induction equation, but concluded that the effect is of at most marginal importance in real galaxies. Chiba & Lesch (1994) developed this idea further and claimed that radial inflow can significantly enhance (if not explain completely) magnetic fields in galaxies. We show here that radial flows in fact hinder dynamo action, and so any enhancement of this type can only be possible as the result of magnetic field transport from infinity, rather than as the result of dynamo action.

Send offprint requests to: D. Moss

Disc dynamos with a radial velocity were considered by Pudritz (1981a,b), Stepinski & Levy (1990) and Mangalam & Subramanian (1994a,b) in the context of accretion discs. Mangalam & Subramanian solved an equation similar to Eq. (11) below, but paid no attention to the specific effects of radial motions on the dynamo efficiency.

Accretion flows driven by dynamo generated magnetic fields, and axisymmetric mean-field galactic dynamos with radial inflow were discussed by Rüdiger et al. (1993) who obtained inward velocities of the order $1\,\mathrm{km\,s}^{-1}$ or less (assuming a speed of sound of $10\,\mathrm{km\,s}^{-1}$) and argued that the sign of v_r depends on the field parity – even or odd in z. (It is not quite clear to us why the sign of v_r can depend on the field parity since magnetic stress is quadratic in the field.) However, these authors neglect the contribution to v_r of the gravitational torques from galactic spiral arms, which is expected to be dominant (see Sect. 2). Their numerical model did not allow these authors to isolate the effects of the radial motions on the dynamo, which are our subject here.

Radial inflow has been invoked to explain strong vertical magnetic fields observed in the Galactic centre by advection of a frozen-in external magnetic field by an accretion flow (Chandran et al. 2000; Sofue 1987). However, the assumption of ideal MHD used by these authors is highly controversial when applied to a large-scale magnetic field in a turbulent galactic disc. The advection of external magnetic field through a turbulent, dynamo active disc will be addressed elsewhere (Moss & Shukurov 2000).

In this paper we include radial motions in a galactic dynamo model and demonstrate that they tend to suppress dynamo action. Without any significant field at infinity (the appropriate condition for a dynamo system), the dynamo has to replenish magnetic field advected by the radial flow away from the region where it is generated most efficiently; this hampers the dynamo action. Magnetic field compression, described by the term $\boldsymbol{B}(\nabla\cdot\boldsymbol{v})$ in the induction equation cannot counterbalance this effect. A noticeable effect of the compression is to produce a sharper peak in magnetic field strength at smaller radii. We consider kinematic mean-field dynamo models and only briefly discuss nonlinear behaviour. We often use values of relevant parameters that are roughly appropriate for the Galaxy. How-

ever, our results are directly applicable to accretion discs after obvious modifications.

2. Radial flows in spiral galaxies

A major mechanism of accretion in spiral galaxies is the non-axisymmetric gravitational torque produced by stellar density waves, which results in an accretion rate $\dot{M} = 0.2$–$0.3 M_\odot\,\mathrm{yr}^{-1}$ (Lubow et al. 1986), corresponding to a radial velocity of $v_r \simeq -0.4\,\mathrm{km\,s}^{-1}$ near the Sun. The viscous stress (Lynden-Bell & Pringle 1974) provides $\dot{M} = 4\pi\nu\sigma \simeq 0.05\,M_\odot\,\mathrm{yr}^{-1}$, where $\nu \simeq 10^{26}\,\mathrm{cm^2\,s}^{-1}$ is the turbulent viscosity and $\sigma \simeq 13\,M_\odot\,\mathrm{pc}^{-2}$ is the gas surface density (with equal contributions from the cold and warm phases of the interstellar medium and $4\,M_\odot\,\mathrm{pc}^{-2}$ from molecular hydrogen) (cf. Sanders et al. 1984, Lacey & Fall 1985). Stress due to the random magnetic field plausibly provides an inflow rate comparable to that of the viscous stresses. Stress produced by the regular magnetic field drives inflow at a rate $\dot{M} = B_r B_\phi H/\Omega \simeq 0.06\,M_\odot\,\mathrm{yr}^{-1}$, where we have taken $B_\phi = 5\,\mu$G, $B_r/B_\phi = 1/4$, $H = 200\,\mathrm{pc}$ (an effective scale height of the gas in the warm and cold phases), and $\Omega = 220\,\mathrm{km\,s}^{-1}/8.5\,\mathrm{kpc}$. Thus, gravitational torques would appear to be the major mechanism driving inflow in the Solar vicinity.

One more source of radial flows in the galactic discs, important for the chemical evolution of spiral galaxies, is the infall of metal-poor gas that has angular momentum different from the local equilibrium value in the disc (Mayor & Vigroux 1981; Lacey & Fall 1985; Pitts & Tayler 1989, 1996; Chamcham & Tayler 1994). The resulting radial velocity within the Solar orbit can be of order $v_r \simeq -1\,\mathrm{km\,s}^{-1}$ (Lacey & Fall 1985, Pitts & Tayler 1996).

Sakhibov & Smirnov (1987, 1989) have analyzed gas velocities in a few spiral galaxies, inferring inflow at azimuthally averaged velocities of $v_r = -(3$–$13)\,\mathrm{km\,s}^{-1}$ at $r = 5$–$9\,\mathrm{kpc}$ in M81, $v_r \simeq -16\,\mathrm{km\,s}^{-1}$ at $r = 4\,\mathrm{kpc}$ in a barred galaxy NGC 925, and an even stronger inflow in NGC 6643 (Sakhibov & Smirnov 1990); an outflow at a velocity $13\,\mathrm{km\,s}^{-1}$ at $r = 4\,\mathrm{kpc}$ was found in the galaxy NGC 2903 (Sakhibov & Smirnov 1990). These velocities are noticeably larger than those implied by the above estimates. Persistent inflow at a velocity of the order of $10\,\mathrm{km\,s}^{-1}$ would result in an accretion rate of about $10\,M_\odot\,\mathrm{yr}^{-1}$ with associated depletion of the interstellar gas within $10^9\,\mathrm{yr}$ or less. The values of $v_r = -(0.5$–$1)\,\mathrm{km\,s}^{-1}$ resulting from theoretical estimates discussed above appear to be more plausible for galaxies where deviations from axial symmetry are not strong. However, radial velocities of order 10–$30\,\mathrm{km\,s}^{-1}$ or more may occur in a galaxy with a strongly non-axisymmetric velocity field, e.g., a barred galaxy (cf. Sect. 5.1).

Little is known about radial profiles of the radial velocities in spiral galaxies. A crude model, applicable at $r \gtrsim 4\,\mathrm{kpc}$, can be obtained by assuming that the gas surface density decreases exponentially with galactocentric radius with a radial scale of about $k^{-1} \simeq 5\,\mathrm{kpc}$ (cf. Lacey & Fall 1985). Assuming that $\dot{M}$ is independent of radius (and thus neglecting star formation and infall), so that $v_r = \dot{M}/(2\pi r\sigma)$, this yields

$$v_r = -1.4\,\mathrm{km\,s}^{-1} e^{k(r-R_\odot)} \left(\frac{r}{R_\odot}\right)^{-1} \left(\frac{\dot{M}}{1\,M_\odot\,\mathrm{yr}^{-1}}\right). \quad (1)$$

Barred galaxies are notable for stronger radial flows resulting from pronounced deviations of the stellar mass distribution from axial symmetry in the bar region. These result in mass inflow at a rate of 2–$4\,M_\odot\,\mathrm{yr}^{-1}$ (Athanassoula 1992); in the inner parts of the bar, $r \lesssim 1\,\mathrm{kpc}$, magnetic stress may play a rôle in driving the inflow (Beck et al. 1999). Inflow at this rate may significantly affect dynamo action in barred galaxies, although stronger shearing of magnetic field by nonaxisymmetric flows typical of barred galaxies can alter the nature of the dynamo even more profoundly.

3. The effect of accretion flows on disc dynamos

In this section we extend the standard asymptotic analysis for mean-field dynamo in a thin disc, valid for small aspect ratios $\lambda = h/r_0$, to include the effects of a prescribed radial flow. Here h and r_0 are the semi-thickness (assumed for convenience to be uniform) and characteristic radius of the ionized gas disc, respectively. (Note that $h \simeq 500\,\mathrm{pc}$ is significantly larger than the scale height of the denser, neutral components of the interstellar gas whose effective scale height is $H \simeq 200\,\mathrm{pc}$.) The analysis is presented in Chapter VII of Ruzmaikin et al. (1988), and we only give an outline here and focus on the inclusion of a radial velocity in the model.

The standard mean field dynamo equation is

$$\frac{\partial \boldsymbol{B}}{\partial t} = \nabla \times (\boldsymbol{v} \times \boldsymbol{B} + \alpha \boldsymbol{B} - \eta \nabla \times \boldsymbol{B})\,, \quad (2)$$

where α and η are the usual mean field coefficients quantifying the alpha effect and turbulent magnetic diffusion, and $\boldsymbol{v}$ and $\boldsymbol{B}$ are the large-scale velocity and magnetic fields. We write $\boldsymbol{v} = r\Omega(r)\widehat{\boldsymbol{\phi}} + v_r(r)\widehat{\boldsymbol{r}}$, with respect to cylindrical polar coordinates (r, ϕ, z). Only axisymmetric solutions will be considered, so that $\partial/\partial\phi = 0$. In this case we can put $\boldsymbol{B} = B_\phi\widehat{\boldsymbol{\phi}} + \nabla \times (A_\phi\widehat{\boldsymbol{\phi}})$.

Eq. (2) is nondimensionalized in the conventional manner (cf. Ruzmaikin et al. 1988) by measuring z, r and t in units of h, r_0 and h^2/η respectively; v_r, Ω and α are measured in units of typical values v_0, Ω_0 and α_0. We also define a unit magnetic field B_0 and unit vector potential $R_\alpha B_0 h$ (with $R_\alpha = \alpha_0 h/\eta$), so that Eq. (2) then splits into the following two scalar equations in terms of the dimensionless variables where, for convenience, we use the $\alpha\omega$ approximation:

$$\frac{\partial B_\phi}{\partial t} = -Dg\frac{\partial A_\phi}{\partial z} + \frac{\partial^2 B_\phi}{\partial z^2} + \lambda^2 \frac{\partial}{\partial r}\left[\frac{1}{r}\frac{\partial}{\partial r}(rB_\phi)\right] - \lambda R_v \frac{\partial}{\partial r}(v_r B_\phi)\,, \quad (3)$$

$$\frac{\partial A_\phi}{\partial t} = \alpha B_\phi + \frac{\partial^2 A_\phi}{\partial z^2} + \lambda^2 \frac{\partial}{\partial r}\left[\frac{1}{r}\frac{\partial}{\partial r}(rA_\phi)\right] - \lambda R_v \frac{v_r}{r}\frac{\partial}{\partial r}(rA_\phi)\,. \quad (4)$$

Here $D = \alpha_0\Omega_0 h^3/\eta^2$ is the dynamo number, $R_v = v_0 h/\eta$ and $g = r d\Omega/dr$.

Now transform variables, with

$$(B_\phi, A_\phi) = (\widetilde{B}_\phi, \widetilde{A}_\phi) \exp\left(\frac{R_v}{2\lambda}\int_0^r v_r(r')\,dr'\right), \quad (5)$$

so that Eqs. (3) and (4) reduce to

$$\frac{\partial \widetilde{B}_\phi}{\partial t} = -Dg\frac{\partial \widetilde{A}_\phi}{\partial z} + \frac{\partial^2 \widetilde{B}_\phi}{\partial z^2} + \lambda^2 \frac{\partial}{\partial r}\left[\frac{1}{r}\frac{\partial}{\partial r}(r\widetilde{B}_\phi)\right] + \widetilde{B}_\phi\left(-\tfrac{1}{4}R_v^2 v_r^2 + \tfrac{1}{2}\lambda R_v \frac{v_r}{r} - \tfrac{1}{2}\lambda R_v \frac{\partial v_r}{\partial r}\right), \quad (6)$$

$$\frac{\partial \widetilde{A}_\phi}{\partial t} = \alpha\widetilde{B}_\phi + \frac{\partial^2 \widetilde{A}_\phi}{\partial z^2} + \lambda^2 \frac{\partial}{\partial r}\left[\frac{1}{r}\frac{\partial}{\partial r}(r\widetilde{A}_\phi)\right] + \widetilde{A}_\phi\left(-\tfrac{1}{4}R_v^2 v_r^2 - \tfrac{1}{2}\lambda R_v \frac{v_r}{r} + \tfrac{1}{2}\lambda R_v \frac{\partial v_r}{\partial r}\right). \quad (7)$$

We now consider solutions with exponential time dependence and set

$$\widetilde{B}_\phi = Q(r)b(r,z)\exp(\Gamma t)\ , \quad \widetilde{A}_\phi = Q(r)a(r,z)\exp(\Gamma t)\ , \quad (8)$$

a form characteristic of dynamo solutions in a thin disc (Ruzmaikin et al. 1988; see Priklonsky et al. 2000 for a comprehensive treatment). In order to obtain a consistent equation for $Q(r)$, i.e. so that Eqs. (6) and (7) both lead to the same equation for Q, we require that a and b satisfy

$$\gamma(r)b = -Dg\frac{\partial a}{\partial z} + \frac{\partial^2 b}{\partial z^2} + \tfrac{1}{2}\lambda R_v\left(\frac{v_r}{r} - \frac{\partial v_r}{\partial r}\right)b\ , \quad (9)$$

$$\gamma(r)a = \alpha b + \frac{\partial^2 a}{\partial z^2} - \tfrac{1}{2}\lambda R_v\left(\frac{v_r}{r} - \frac{\partial v_r}{\partial r}\right)a\ , \quad (10)$$

so that

$$\Gamma Q = \widetilde{\gamma}(r)Q + \lambda^2\frac{d}{dr}\left[\frac{1}{r}\frac{d}{dr}(rQ)\right]\ , \quad (11)$$

where

$$\widetilde{\gamma}(r) = \gamma(r) - \tfrac{1}{4}R_v^2 v_r^2\ . \quad (12)$$

Eqs. (9) and (10) can be considered as describing local dynamo action in a uniform slab, with g, α, v_r and $\partial v_r/\partial r$ evaluated at a radius r; then $\gamma(r)$ is the local growth rate. These equations reduce to those given in Ruzmaikin et al. (1988) when $R_v = 0$.

The last terms on the right-hand sides of the local equations (9) and (10) are λ^{-1} times smaller than the remaining terms and we show in Appendix A that it only gives a perturbation of order λ^2 to the local growth rate γ. Since $\lambda \ll 1$, their effect on the local dynamo action is relatively small. In the thin-disc approximation discussed in this section, the magnetic pitch angle p is determined from the ratio of the dimensional field components resulting from the local problem, $\tan p = R_\alpha B_r/B_\phi = -R_\alpha h(\partial a/\partial z)/b$. Therefore the main effect of the $O(\lambda)$ terms in the local equations will be on the pitch angle; it is shown in Appendix A that the effect on p (whose magnitude is of order λ) is sensitive to the radial profile of v_r.

The effect of the radial motions on the disc dynamo is now clear. If the boundary conditions are $B_\phi, A_\phi = 0$ at $r = 0$ and $r = 1$, then $\widetilde{B}_\phi, \widetilde{A}_\phi$ satisfy the same boundary conditions, and Eq. (11) is formally identical to a standard (i.e., with $R_v = 0$) radial dynamo equation, but with $\widetilde{\gamma}$ replacing γ. Thus for $R_v = O(1)$, the effective local growth rate $\widetilde{\gamma}$ in Eq. (11) is significantly reduced at all radii from that of the standard solution. It is obvious from Eq. (12) that the effect acts on γ at zero order in λ, and thus also at zero order on Γ – see Eq. (11). We can demonstrate (see Appendix A) that the last terms in Eqs. (9) and (10) enhance the dynamo action, but their effect is weaker, of order λ^2. Thus the overall effect of a radial flow with $R_v = O(1)$ will be to decrease the global growth rate Γ in a disc of small or moderate thickness. Note that the lowest order effect is quadratic in v_r, so both inflow and outflow tend to suppress the dynamo.

In the next section we consider the effects of radial motions on disc dynamos using another approximate method, and find reasonable agreement with the above arguments.

4. A simplified numerical model

We compare the prediction of Sect. 3 that radial motions tend to suppress the dynamo with the results from a simple explicit numerical model of a dynamo in a thin disc $0 \le r \le R$ of half-thickness h, using the 'no-z' approximation of Moss (1995), where we replace z-derivatives by inverse powers of h in Eqs. (3) and (4) and note that $B_r = -\partial A_\phi/\partial z$ (see also Subramanian & Mestel 1993). The code is described in Moss (1995), and represents a different scheme of approximation to that of Sect. 3. It applies to solutions that are even with respect to the midplane (quadrupole-like), and is consistent with vacuum boundary conditions at the surface of the disc, $|z| = h$. The relation of this approximation to that of Sect. 3 is discussed by Phillips (2000).

We restrict our attention to axisymmetric solutions, and take a Brandt rotation law

$$\Omega = \frac{\Omega_0}{[1 + (r/r_\omega)^2]^{1/2}}\ , \quad (13)$$

with $r_\omega = 0.2R$. We assume that α ($= \alpha_0$) and η are uniform with respect to radius. Following nondimensionalization using a time unit h^2/η and length unit R, the dynamo equation (2) becomes

$$\frac{\partial B_r}{\partial t} = -\lambda R_v\frac{v_r}{r}\frac{\partial}{\partial r}(B_r r) - R_\alpha B_\phi - B_r + \lambda^2\frac{\partial}{\partial r}\left[\frac{1}{r}\frac{\partial}{\partial r}(rB_r)\right],$$

$$\frac{\partial B_\phi}{\partial t} = -\lambda R_v\frac{\partial}{\partial r}(v_r B_\phi) + R_\omega r B_r\frac{\partial \Omega}{\partial r} - B_\phi + \lambda^2\frac{\partial}{\partial r}\left[\frac{1}{r}\frac{\partial}{\partial r}(rB_\phi)\right],$$

where $\lambda = h/R$. Similarly to Sect. 2, the dynamo numbers are defined as $R_\alpha = \alpha_0 h_0/\eta$, $R_\omega = h^2\Omega_0/\eta$, and $R_v = v_0 h/\eta$. With typical values $\eta = 10^{26}\,\mathrm{cm^2\,s^{-1}}$ and $h = 500\,\mathrm{pc}$, $R_v = 1$ corresponds to $v_0 \approx 0.7\,\mathrm{km\,s^{-1}}$.

In the no-z model, B_r and B_ϕ are to be regarded as averages over z at given radius, or as representative mid-plane

Table 1. Growth (decay) rates of the leading even, axisymmetric mode for the 'no-z' model with radial velocity profiles (14)– (17), $r_\omega = 0.2$; an asterisk indicates that the spatial resolution was becoming inadequate near $r = 0$. Blank entries indicate that no calculation was performed for those parameter values.

R_v	-3	-2	-1	0	1	2	3	5	6	10
Case 1	-0.18	0.23	0.63	0.80	0.63	0.24	-0.17			
Case 2				0.80	0.73	0.60	0.48			-0.14^*
Case 3				0.80	0.80		0.795			0.785^*
Case 4				0.80	0.75			0.16	-0.01	

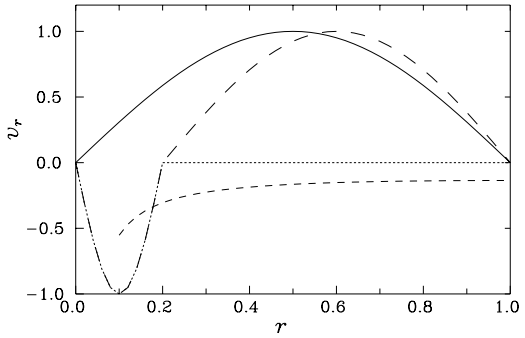

Fig. 1. The model radial velocity profiles: Case 1, Eq. (14) (solid); Case 2, Eq. (15) (long-dashed); Case 3, Eq. (16) (dotted); and Case 4, Eq. (17) (short-dashed)

values, in contrast to the asymptotic analysis where B_ϕ and A_ϕ are functions of z. Note the different definitions of the dimensionless radial magnetic field between this section and Sect. 3: the variable here denoted B_r is equal to $R_\alpha B_r$ of Sect. 3. However, for our model where $R_\alpha \approx 1$, this distinction is of minor importance.

Boundary conditions $B_r = B_\phi = 0$ are applied at the outer boundary $r = 1$. The boundary conditions in the inner disc are specified below.

We considered several radial velocity profiles v_r shown in Fig. 1, with (in dimensionless form)

$$1.\ v_r = \sin \pi r\ ; \tag{14}$$

$$2.\ v_r = \begin{cases} -\sin(\pi r/r_\omega)\ , & r \le r_\omega\ , \\ \sin[\pi(r-r_\omega)/(1-r_\omega)]\ , & r > r_\omega\ ; \end{cases} \tag{15}$$

$$3.\ v_r = \begin{cases} -\sin(\pi r/r_\omega)\ , & r \le r_\omega\ , \\ 0\ , & r > r_\omega\ , \end{cases} \tag{16}$$

$$4.\ v_r = -0.05 r^{-1} \exp\left(\frac{r}{r_0}\right)\ , \tag{17}$$

with a suitably chosen r_0 (see below). Cases 1–3, see Eqs. (14)–(16), are intended to illustrate in idealized form the main effects of radial flows, and there we took the inner boundary at $r_i = 0$. The velocity field in Case 4, Eq. (17), was chosen to have a resemblance to the more realistic case of Eq. (2), and here we took $r_i = 0.1$, because this simplistic model is not applicable in the inner regions of the Milky Way, and an unrealistically large velocity there could distort our results. The boundary conditions applied at the inner boundary $r = r_i$ are $B_r = B_\phi = 0$ if $r_i = 0$ and $\partial B_r/\partial r = \partial B_\phi/\partial r = 0$ if $r_i > 0$. We also tried a selection of other boundary conditions, including a constant magnetic field at the outer boundary to allow for advection of magnetic flux from infinity. However this never leads to enhancement of magnetic field in the main parts of the disc, as envisaged by Chiba & Lesch (1994), as the dynamo action actively suppresses any externally supplied magnetic field unless, perhaps, the external field is unrealistically strong, or the inflow velocity unrealistically large. These issues are discussed in more detail by Moss & Shukurov (2000).

We first determined (by step by step integration) the linear growth rate, $\Gamma = d \ln |\boldsymbol{B}|/dt$, of the fastest growing eigenmode for a number of values of R_v for the choices of v_r of Cases 1–3. We adopted as standard illustrative values $R_\alpha = 1$, $R_\omega = 10$, $\lambda = 0.05$. (These parameters can be thought of as corresponding to $R = 10\,\mathrm{kpc}$, $\eta = 2 \times 10^{26}\,\mathrm{cm^2\,s^{-1}}$, $\alpha_0 = 1\,\mathrm{km\,s^{-1}}$ and $\Omega_0 = 10^{-15}\,\mathrm{s^{-1}}$, but these examples are intended to be generic, and not to model any specific galaxy.) The results are summarized in Table 1. The spatial resolution was poor for $R_v = 10$, but the eigenvalues still seem to be reasonably reliable, even for this extreme value. In Cases 1 and 2 the outcome is clear – growth rates are significantly reduced when $|R_v| > 0$, and become negative for large enough $|R_v|$. As expected, the effect is insensitive to the sign of R_v. Radial inflow shifts the maximum of an eigenfunction to smaller radii. In Case 3, the same trend is observed, but the magnitude of the effect is much smaller because $v_r \ne 0$ in only a small part of the disc.

As mentioned above, the Case 4 velocity field was chosen to represent a simple model of the galactic inflow. In this case we took $R_\alpha = 1$, $R_\omega = 20$, $\lambda = 1/30$ and $r_0 = 1/3$. The linear results for this model are also given in Table 1; we verified that these results were not sensitive to the boundary condition imposed at $r = r_i$, nor to the value of r_i – taking $r_i = 0.2$, for example, caused no significant changes. The radial dependence of B_r and B_ϕ in the linear eigenmode with $R_v = 0$ and $R_v = 4$ is displayed in the lower panels of Figs. 2 and 3.

We also investigated briefly simple nonlinear solutions for Case 4, taking an alpha-quenching $\alpha \propto (1+\boldsymbol{B}^2)^{-1}$. We show in the lower panels of Figs. 4 and 5 the fields B_r, B_ϕ in the steady state with $R_v = 0$ and 4. As we can see, the displacement of the field toward smaller radii by the inflow occurs also in the nonlinear solutions. Further increasing R_v causes the field to be concentrated still more to smaller radii.

We show in the upper panels of Figs. 2–5 the variation with radius of pitch angle in our linear and nonlinear solutions with a Case 4 radial flow. As expected, the pitch angle is weakly affected by the radial motions, as described by the $O(\lambda)$ terms in

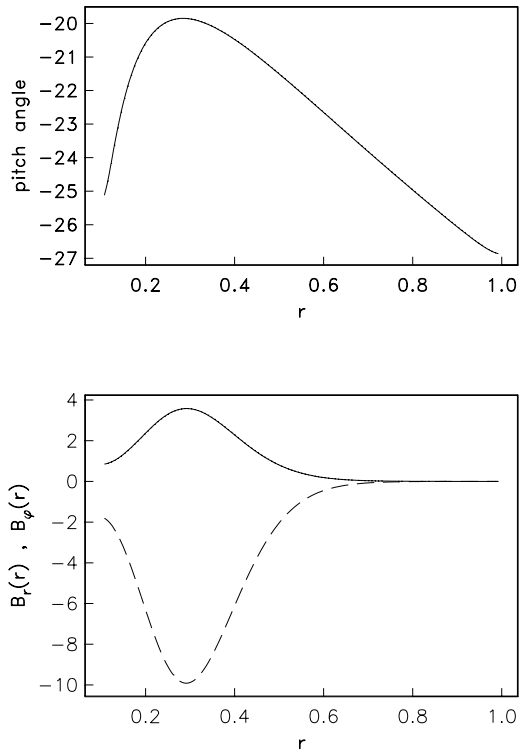

Fig. 2. The 'no-z' model with no radial velocities ($R_v = 0$), linear eigenmode. Upper panel: the pitch angle (in degrees) of the magnetic field. Lower panel: B_r (solid) and B_ϕ (broken).

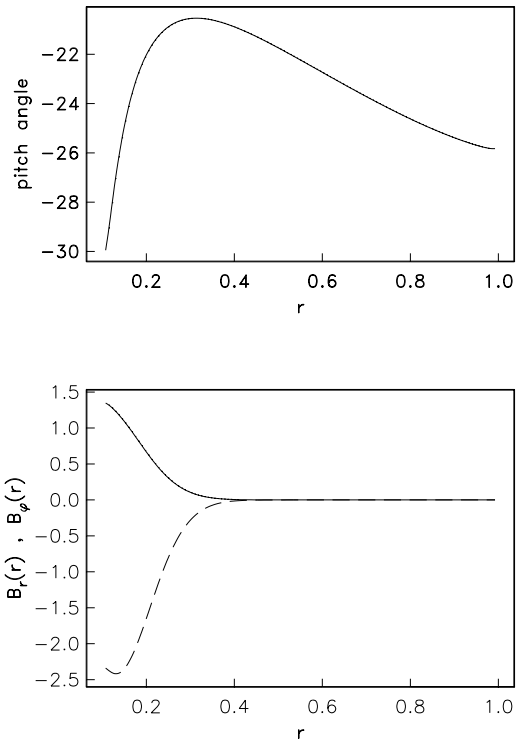

Fig. 3. As Fig. 2, except that the radial velocity profile is that of Case 4, Eq. (17), with $R_v = 4$.

the local equations (9) and (10). The dependence of the pitch angle on the radial profile of v_r in both linear and nonlinear solutions is consistent with the approximate solution of Eqs. (9) and (10) presented in Appendix A. An axisymmetric radial flow cannot enhance the radial magnetic field by stretching the azimuthal one, so the effect is only weak. However, one might expect the pitch angle to be affected more strongly in nonaxisymmetric flows.

We can compare the results from Case 1 with the results of Sect. 3 for the perturbation to the local growth rate $\widetilde{\gamma}(R)$. If we take a mean value of v_r^2 of $\frac{1}{2}$, then $\Delta\widetilde{\gamma} = -(\frac{1}{2}R_v v_r)^2 \approx -\frac{1}{8}$ for $R_v = 1$, compared with $\Delta\Gamma = 0.63$–$0.80 = -0.17$ from the first line in Table 1. This is arguably as good an agreement as could be expected. However, for larger values of R_v, the approximation of Sect. 3 gives a larger reduction of the local growth rate than obtained for the global growth rate with these numerical experiments, that is the dependence of $\Delta\Gamma$ on R_v from the solutions of this section is weaker than $\Delta\Gamma \propto R_v^2$. We should note, however, that Γ is not the same quantity as $\widetilde{\gamma}$, so it does not necessarily follow that Eq. (12) is a poor approximation.

5. Magnetically driven accretion flows

In this section we turn to the question of how accretion flows might be driven by dynamo generated magnetic fields. Moss et al. (1999) modelled the dynamo generation of magnetic fields in a weakly barred galaxy (IC 4214). The striking feature of these fields was the relatively large field strengths locally, associated with regions of gas streaming. The Lorentz forces of these fields were not included in the original dynamical model, but simple estimates given in Sect. 5.2 show that the effects may be significant when $|\boldsymbol{B}| \simeq 10\,\mu\mathrm{G}$, especially because the magnetic field varies on a relatively small horizontal scale of order 1 kpc. This field strength can be reached in the inner regions of spiral galaxies and in the bars of barred galaxies.

5.1. The magnetically driven accretion flow

In order to make a rather more detailed estimate of the velocities driven by the Lorentz forces, we solve the Navier–Stokes equation including only the Lorentz forces associated with the dynamo generated magnetic fields of Moss et al. (1999), together with a scalar turbulent viscosity. In these dynamo solutions an approximately steady field pattern rotates with the gas spiral pattern speed Ω_p. We show in Fig. 6 a snapshot of $\boldsymbol{B}(r,\phi,t)$ at an arbitrarily chosen time.

We take the governing equation for the flow in the form

$$\frac{\partial \boldsymbol{u}}{\partial t} + (\boldsymbol{u}\cdot\nabla)\boldsymbol{u} = \frac{1}{4\pi\rho}(\nabla\times\boldsymbol{B})\times\boldsymbol{B} - \frac{1}{\rho}\nabla p + \nu\nabla\cdot\mathcal{T}, \quad (18)$$

where $\boldsymbol{u}$ denotes the magnetically driven velocities, $\mathcal{T}$ is the rate of strain tensor, and ν is the kinematic diffusivity (assumed constant). We nondimensionalize in terms of a speed U, length R, time R/U, field strength B_0 and density ρ_0, and it is convenient to take $U = 1\,\mathrm{km\,s^{-1}}$, $R = 15\,\mathrm{kpc}$ (the radius of the model galaxy) and $\rho_0 = 10^{-24}\,\mathrm{g\,cm^{-3}}$. We allow for a density that varies with radius, $\rho(r) = \rho_0\widetilde{\rho}$, where $\widetilde{\rho}$ is the dimension-

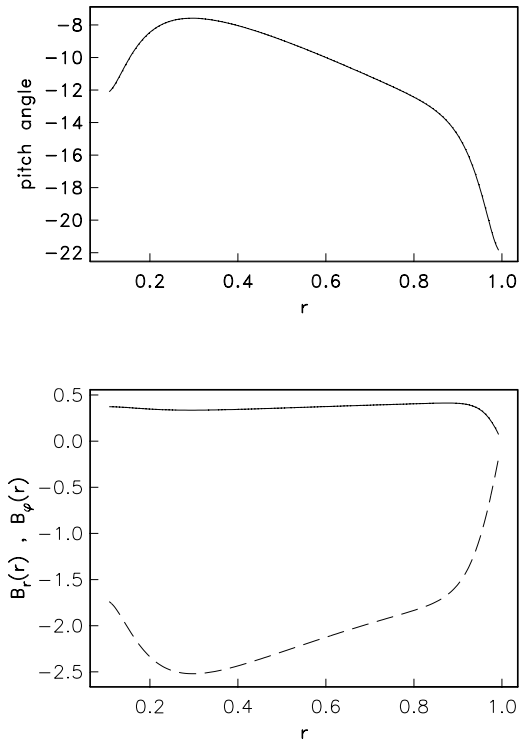

Fig. 4. The 'no-z' model with $R_v = 0$, nonlinear (α-quenched) solution. Upper panel: the pitch angle (in degrees) of magnetic lines. Lower panel: B_r (solid) and B_ϕ (broken).

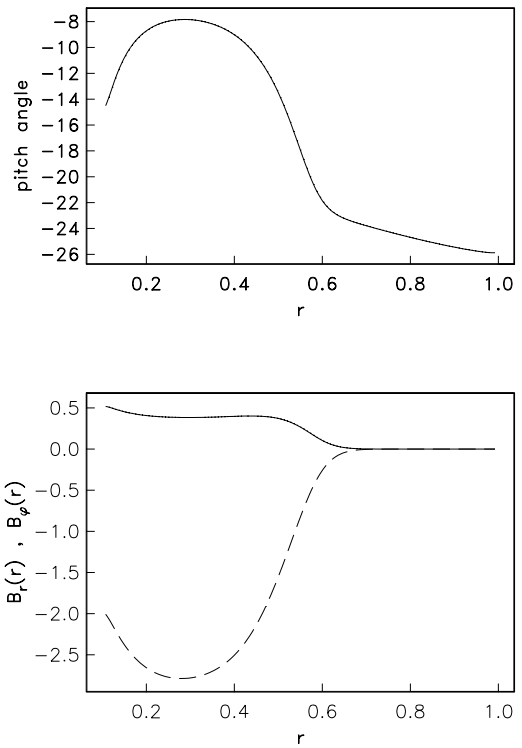

Fig. 5. As Fig. 4, except that the radial velocity profile is that of Case 4, Eq. (17), with $R_v = 4$.

less density. The $\boldsymbol{B}$ values from Moss et al. (1999) are in units of $qB_{\rm eq}$, where $B_{\rm eq}^2 = 4\pi\rho v_{\rm t}^2$ defines the equipartition field strength with ρ and $v_{\rm t}$ the gas density and turbulent velocity, and q is of order unity. These units arise from the alpha-quenching nonlinearity used in that paper. In this model, at radius $7\,{\rm kpc}$ the azimuthally averaged field strength in dimensionless units is about 2, and the maximum (in a very sharp peak) is about 20. At $13\,{\rm kpc}$, the azimuthally averaged field strength is about 5, with only small variations.

We do not have a satisfactory continuum model for the gas because the velocity field results from an N-body simulation, and so cannot readily include the pressure gradient term. We anticipate that the gas pressure gradient will adjust to compensate for the magnetic pressure component of the Lorentz force, but not for the magnetic tension, and that the centrifugal force is balanced by gravity and the total pressure gradient. In this spirit, we ignore the pressure gradient and the centrifugal force terms in Eq. (18), and include only the part of the Lorentz force corresponding to the magnetic tension. (In fact, the omission of the centrifugal force term has very little effect on the solutions.)

Then, in dimensionless variables

$$\frac{\partial u_r}{\partial t} = -u_r\frac{\partial u_r}{\partial r} - \frac{u_\phi}{r}\frac{\partial u_r}{\partial \phi} + \widetilde{\rho}^{-1}\Lambda L_r + \mathcal{R}^{-1}\left(\Delta_{r\phi}u_r - \frac{2}{r^2}\frac{\partial u_\phi}{\partial\phi} - \frac{u_r}{r^2}\right), \quad (19)$$

$$\frac{\partial u_\phi}{\partial t} = -u_r\frac{\partial u_\phi}{\partial r} - \frac{u_\phi}{r}\frac{\partial u_\phi}{\partial \phi} - \frac{u_r u_\phi}{r} + \widetilde{\rho}^{-1}\Lambda L_\phi + \mathcal{R}^{-1}\left(\Delta_{r\phi}u_\phi + \frac{2}{r^2}\frac{\partial u_r}{\partial\phi} - \frac{u_\phi}{r^2}\right), \quad (20)$$

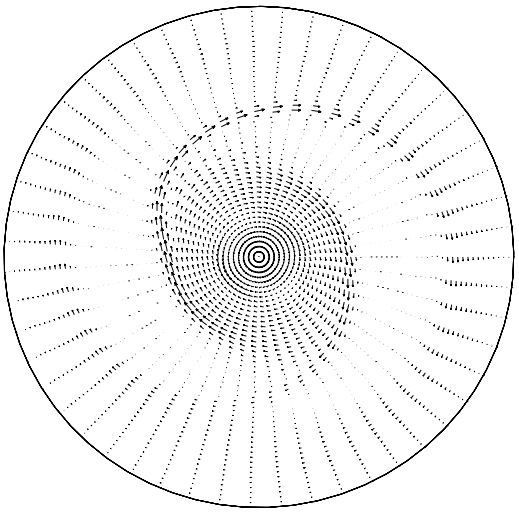

Fig. 6. Snapshot of magnetic field vectors, used in the model of Sect. 5, at an arbitrarily chosen time.

where $\mathcal{R} = UR/\nu$ is the turbulent Reynolds number, $\Delta_{r\phi} = r^{-1}(\partial/\partial r)(r\partial/\partial r) + r^{-2}\partial^2/\partial\phi^2$, $\Lambda = B_0^2/(4\pi U^2\rho_0)$, and $\boldsymbol{L} = \boldsymbol{B}\cdot\nabla\boldsymbol{B}$ is the dimensionless magnetic tension. We recognize that in a more consistent nonlinear treatment the zero order velocities of the nonmagnetic dynamical simulation should also be included, but as they were not derived from a continuum hydrodynamical model, this was not practical. Thus we regard the

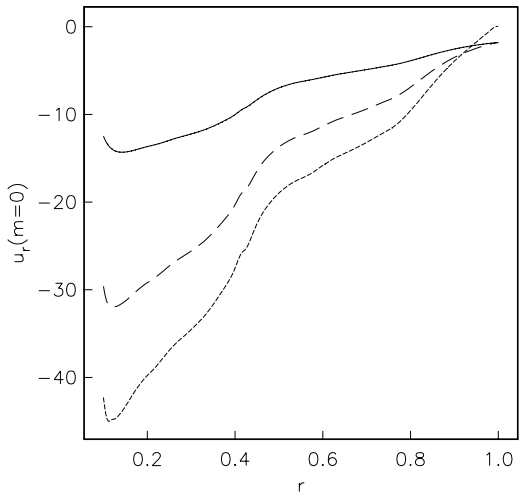

Fig. 7. The radial dependence of the axisymmetric ($m = 0$) component of the radial velocity (in $\mathrm{km\,s^{-1}}$) in a model with nonuniform density for $\dot{M} = 3\,M_\odot\,\mathrm{yr}^{-1}$ and $\Lambda = 10$ (solid) and 30 (dashed), and in a model with uniform density for $\Lambda = 30$ (short-dashed).

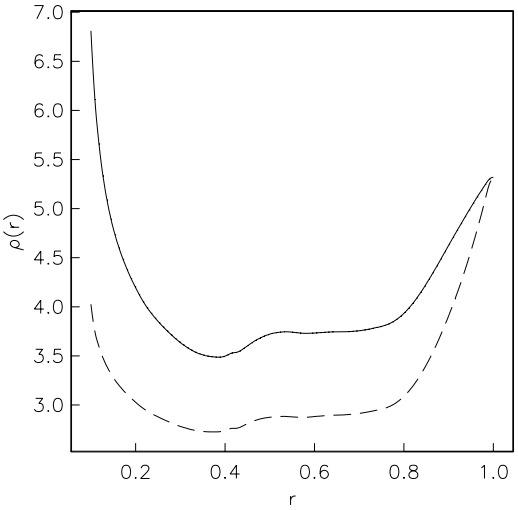

Fig. 8. The radial dependence of density (in units of $10^{-24}\,\mathrm{g\,cm^{-3}}$) for $\dot{M} = 3\,M_\odot\,\mathrm{yr}^{-1}$: $\Lambda = 10$ (solid), $\Lambda = 30$ (dashed).

solution of Eqs. (19) and (20) as just giving an indication of the gross effects of including the Lorentz force.

When $\nu = 2 \times 10^{26}\,\mathrm{cm^2\,s^{-1}}$ (equal to the value of the turbulent magnetic diffusivity in the dynamo calculations), then $\mathcal{R}^{-1} \approx 0.05$. A rather larger value, $\mathcal{R}^{-1} = 0.2$, was used in the calculations reported here, for reasons of numerical convenience, but the solutions do not appear to be very sensitive to this choice. For the parameter $\Lambda = q^2 v_\mathrm{t}^2/U^2$, the range $10 \lesssim \Lambda \lesssim 50$ seems to be reasonable, taking the typical estimate of $v_\mathrm{t} \simeq 10\,\mathrm{km\,s^{-1}}$. Boundary conditions are either that $u_r = 0$ at $r = r_\mathrm{min}$ and $r = 1$, or are 'open', with $u_r \propto r$ at $r = r_\mathrm{min}$ and $\partial(r u_r)/\partial r = 0$ at $r = 1$. Also $u_\phi = 0$ at $r = r_\mathrm{min}$ and $r = 1$.

The field pattern $\boldsymbol{B}$ rotates with the pattern speed $\Omega_\mathrm{p} = 37.3\,\mathrm{km\,s^{-1}\,kpc^{-1}}$, and is steady in the rotating frame. Note that $|\boldsymbol{B}|$ has a marked spiral structure at larger radii (outside of the corotation radius), but is less pronouncedly nonaxisymmetric within this radius. The pitch angle becomes smaller, and the magnetic arms broader, as radius increases, and so *inter alia* for a given field strength in the arms the azimuthally averaged strength will increase with radius, for purely geometrical reasons. By timestepping Eqs. (19) and (20), we computed solutions that were oscillating at low amplitude in the rotating frame, for $\Lambda = 10,\ 30$ and 50.

First we considered the rather unrealistic case of uniform density, $\widetilde{\rho} = 1$. This simplification might be justified to a degree by noting that the scale of variation of ρ is rather greater than that of $|\boldsymbol{B}|$ (see Moss et al. 1999). Also, the effects of an inhomogeneous density will be to decrease $|\boldsymbol{u}|$ where $\rho > \bar{\rho}$ and to decrease it where $\rho < \bar{\rho}$, with $\bar{\rho}$ the mean density. Our interest is in the accretion rate, given by the azimuthally averaged radial velocity, which we might expect would not be strongly affected by this approximation. For each value of Λ considered, the flow is everywhere close to radial and inwardly directed, except perhaps very close to $r = 1$. (The boundary condition $\boldsymbol{B} = 0$ at $r = 1$ imposed on the dynamo solution may distort somewhat the solution near this boundary.) The azimuthally averaged ($m = 0$ Fourier component) of the magnetically driven radial velocity u_r for $\Lambda = 30$, open boundary conditions and $r_\mathrm{min} = 0.1$, is shown as a function of r in Fig. 7. Solutions are insensitive to the value of r_min and are not significantly affected by change of boundary conditions.

These models are inconsistent in that they imply a mass inflow rate that varies with radius or, alternatively, they cannot truly be near to a steady flow state. Thus we also examined models in which we took a constant mass inflow rate throughout the disc, and determined the density by $\rho = \rho_b - \dot{M}/(4\pi r \langle u_r \rangle H)$, where $\langle u_r \rangle$ is the azimuthally averaged radial velocity, H is the scale height for the gas distribution, and ρ_b represents a 'background' gas density, generated by effects that we do not include here, such as gravitational torques, infall from the halo, etc. Rather arbitrarily, we took $\rho_b = \rho_0$ for illustrative purposes. Models were calculated for several values of Λ and $\dot{M}$, taking $r_\mathrm{min} = 0.1$ with open boundary conditions. The general nature of the solutions was quite similar to those found previously assuming that density was constant. We show in Fig. 7 the radial dependence of $\langle u_r \rangle$ for models with $\dot{M} = 3\,M_\odot\,\mathrm{yr}^{-1}$, $\Lambda = 10$ and 30. In Fig. 8 we give the function $\widetilde{\rho}(r)$ for these cases. The azimuthally averaged values of the radial velocity of some tens of $\mathrm{km\,s^{-1}}$ are consistent with our estimates presented below. $\rho(r)$ is dominated by the effects of the magnetically driven accretion flow, i.e. ρ is significantly greater than ρ_b ($\widetilde{\rho}$ larger than 1), which is arguably unrealistic. Increasing ρ_b would decrease the infall velocities, but we did not attempt to pursue this point, in view of the other major simplifications present in what is only intended to be an illustrative model. There is also a more fundamental point, that in a truly self-consistent solution, the accretion rate $\dot{M}$ would be determined simultaneously with the flow velocity field (rather than being prescribed). We did not pursue this further in what is intended as only a first approximation to a solution.

5.2. The accretion rate

We can estimate a typical mass accretion rate, taking a radius of 10 kpc, mean radial velocity $-10\,\mathrm{km\,s^{-1}}$, $\rho = 10^{-24}\,\mathrm{g\,cm^{-3}}$, $H = 0.2\,\mathrm{kpc}$, giving $\dot{M} \simeq 3\,M_\odot\,\mathrm{yr^{-1}}$. This value is comparable to those required to feed the central activity in barred galaxies (Shlosman et al. 1990; Regan et al. 1997). This confirms and extends the earlier conclusion of Beck et al. (1999) that magnetic stresses may be important in angular momentum transfer in barred galaxies.

The accretion rate from magnetic stresses in our simulations is significantly larger than the estimates of Sect. 2 which apply to axially symmetric magnetic fields. The difference is due to strong deviations of the magnetic field from axial symmetry at scales smaller the those of the local velocity field. This difference in the local scales results from rapid advection of magnetic field from regions of strong velocity shear. So, if l_v is the scale of the velocity field and l_B is that of magnetic field, then the velocity resulting from $|\rho\boldsymbol{u}\cdot\nabla\boldsymbol{u}| \simeq |(\nabla\times\boldsymbol{B})\times\boldsymbol{B}/(4\pi)|$ is $u \simeq 30\,\mathrm{km\,s^{-1}}$ for $l_B/l_v = 5$ (consistent with our model), $B = 10\,\mu\mathrm{G}$ and $\rho = 10^{-24}\,\mathrm{g\,cm^{-3}}$. This estimate is of the same order as that found in the above simulations, see Fig. 7.

6. Discussion

The suppression of the dynamo action by radial velocities (both directed inward and outward) produces a negative feedback on the dynamo. In principle, the dynamo action might be saturated by this feedback alone. For illustration assume that $\gamma \simeq (h^2/\eta)^{-1}$. Using Eq. (12), the dynamo is saturated when $\widetilde{\gamma} = 0$, or $v_r \simeq 2\eta/h \simeq 1\,\mathrm{km\,s^{-1}}$. Attributing this velocity to the magnetic field alone, we obtain from

$$v_r \simeq \frac{1}{4\pi}\,\frac{B_r B_\phi}{\rho r\Omega}$$

the corresponding steady-state field strength as

$$B_\phi \sim 10\,\mu\mathrm{G}\ ,$$

where we took $B_r/B_\phi \simeq 1/4$, $\rho \simeq 10^{-24}\,\mathrm{g\,cm^{-3}}$ and $r\Omega = 200\,\mathrm{km\,s^{-1}}$ as typical of the Solar neighbourhood. The resulting estimate of the magnetic field is only slightly larger than that observed in the outer parts of spiral galaxies. This indicates that this nonlinear effect may contribute significantly to the saturation of the dynamo, especially in the inner parts of galaxies. If v_r grows inward as r^{-1}, the dynamo saturation due to accretion can become significant at $r \simeq 3\,\mathrm{kpc}$ if $v_r = 1\,\mathrm{km\,s^{-1}}$ at the Solar radius. The effect of the radial motions on the dynamo might be expected to be stronger in galaxies with stronger and more open spiral patterns and in barred galaxies.

There are several nonlinear mechanisms known that lead to the saturation of the mean field dynamo action in galaxies independently of the traditionally invoked alpha quenching. These include inflation of the galactic disc by the magnetic field (Dobler et al. 1996), magnetic buoyancy (Moss et al. 1999), magnetically driven accretion (this paper).

Even though each individual mechanism may be weaker than alpha quenching is believed to be, together they may be able to saturate the dynamo more efficiently.

Acknowledgements. We acknowledge support from NATO Collaborative Linkage Grant PST.CLG 974737. DS is grateful to the Royal Society for financial support, and to the University of Newcastle for its hospitality.

Appendix A: expansion in free decay modes for the local dynamo equations

In order to substantiate the discussion of the effects of radial velocity on the local dynamo modes, we present here an approximate solution of Eqs. (9) and (10) in the form of series expansions in free decay modes, $b_n(z)$ and $a_n(z)$, satisfying

$$\gamma_n b_n = b_n''\ , \qquad \gamma_n a_n = a_n''\ ,$$

where $\gamma_n\ (<0)$ is the decay rate of the nth mode and a prime denotes a derivative with respect to z. For the sake of definiteness, we choose boundary conditions that select quadrupolar modes (see, e.g., Ruzmaikin et al. 1988),

$$b_n'(0) = b_n(1) = a_n(0) = a_n'(1) = 0\ .$$

The resulting orthonormal set of basis functions is given by

$$\begin{pmatrix} b_{2n} \\ a_{2n} \end{pmatrix} = \begin{pmatrix} \sqrt{2}\cos\frac{1}{2}\pi(2n+1)z \\ 0 \end{pmatrix},$$

$$\begin{pmatrix} b_{2n+1} \\ a_{2n+1} \end{pmatrix} = \begin{pmatrix} 0 \\ \sqrt{2}\sin\frac{1}{2}\pi(2n+1)z \end{pmatrix},$$

$$\gamma_{2n} = \gamma_{2n+1} = -\tfrac{1}{4}\pi^2(1+2n)^2\ , \quad n = 0, 1, \ldots\ .$$

Note that the free decay eigenvalues are all doubly degenerate, and two vector eigenfunctions correspond to each eigenvalue, one with $b_n = 0$, and the other with $a_n = 0$. The eigenfunctions are normalized to have $\int_0^1 (b_n^2 + a_n^2)\,dz = 1$.

The solution of Eqs. (9) and (10) is represented as

$$\begin{pmatrix} b \\ a \end{pmatrix} \approx \exp(\gamma t)\sum_{n=0}^{N} c_n \begin{pmatrix} b_n \\ a_n \end{pmatrix},$$

where N is chosen to achieve the required accuracy of the solution. We substitute this series into Eqs. (9) and (10), multiply by $(b_k,\ a_k)$ and integrate over z from 0 to 1 to obtain an algebraic system of homogeneous equations for c_k whose solvability condition yields an algebraic equation for γ. For our current purposes, it is sufficient to retain the smallest possible number of modes, which results in a system of two equations for c_0 and c_1 and a quadratic equation for γ whose positive solution is given by

$$\gamma \approx -\tfrac{1}{4}\pi^2 + \left(W_{01}W_{10} + \lambda^2 L_v^2\right)^{1/2}\ , \tag{A.1}$$

where

$$W_{01} \ = \ -\int_0^1 \alpha b_0 a_1\,dz = -\tfrac{1}{2} \quad \text{for } \alpha = \sin\pi z\ ,$$

$$W_{10} \;=\; D\int_0^1 b_0 a_1\, dz = \frac{2}{\pi} D\;,$$
$$L_v \;=\; \tfrac{1}{2} R_v \left(\frac{v_r}{r} - \frac{\partial v_r}{\partial r} \right).$$

To assess the accuracy of Eq. (A.1), we note that it yields $\gamma = 0$ for $D = -\pi^5/16 \approx -19$ if $R_v = 0$, as compared with the accurate value of about -8.

As we can see, radial motions enhance the local dynamo action via the positive definite term $\lambda^2 L_v^2$ in Eq. (A.1), but the effect is only quadratic in λ. Therefore, this enhancement cannot overcome the suppression resulting from the radial dynamo equation, evident from Eq. (12). Indeed, the increment in γ resulting from Eq. (A.1) is of the order of $\frac{1}{8}(-\pi/D)^{1/2}\lambda^2 R_v^2 v_r^2/r^2$ for $\lambda|R_v/D| \ll 1$, and this is smaller than the decrement resulting from Eq. (12), $-\frac{1}{4}R_v^2 v_r^2$, provided $\lambda^2/r^2 \lesssim 2(-\pi/D)^{1/2} \simeq 1$, i.e., whenever the thin-disc approximation employed here is applicable. We conclude that radial motions, both inflow and outflow, suppress dynamo action in a disc of small or moderate thickness.

The effect of the radial motions of the pitch angle of magnetic field p is obvious from

$$\tan p \;=\; \frac{b_r}{b_\phi} = -\frac{R_\alpha a'}{b} \approx -\frac{\pi c_1}{2c_0}$$
$$\approx -\tfrac{1}{2}\pi^{3/2}\frac{R_\alpha}{\sqrt{-D}}\left(1 - \tfrac{1}{2}\lambda L_v \sqrt{\frac{\pi}{-D}}\right),$$

where the last equality applies for $\lambda|R_v/D| \ll 1$. So, the magnetic field becomes more azimuthal ($|p|$ decreases) if $v_r/r - \partial v_r/\partial r > 0$, that is if $(n+1)v_r > 0$ for $v_r \propto r^{-n}$. It is remarkable that the radial motions reduce $|b_r/b_\phi|$ for $(n+1)v_r > 0$, i.e., for inflow with $|v_r|$ decreasing with r faster than $1/r$. This tendency is seen in Figs. 2–5 where the inflow makes the field more azimuthal at small radii and more radial at large r. Note that the effect of v_r on the pitch angle may be different for dipolar modes.

References

Athanassoula E., 1992, MNRAS 259, 345
Beck R., Ehle M., Shoutenkov V., Shukurov A., Sokoloff D., 1999, Nat 397, 324
Chamcham K., Tayler R.J., 1994, MNRAS 266, 282
Chandran B.D.G., Cowley S.C., Morris M., 2000, ApJ 528, 723
Chiba M., Lesch H., 1994, A&A 284, 731
Dobler W., Poezd A., Shukurov A., 1996, A&A 312, 663
Lacey C.G., Fall S.M., 1985, ApJ 290, 154
Lubow S.H., Balbus S.A., Cowie L.L., 1986, ApJ 309, 496
Lynden-Bell D., Pringle J.E., 1974, MNRAS 168, 603
Mangalam A.V., Subramanian K., 1994a, ApJ 434, 509
Mangalam A.V., Subramanian K., 1994b, ApJS 90, 963
Mayor M., Vigroux L., 1981, A&A 98, 1
Moss D., 1995, MNRAS 275, 191
Moss D., Shukurov A., 2000, in preparation.
Moss D., Rautiainen P., Salo H., 1999, MNRAS 303, 125
Moss D., Shukurov A., Sokoloff D., 1999, A&A 343, 120
Pitts E., Tayler R.J., 1989, MNRAS 240, 373
Pitts E., Tayler R.J., 1996, MNRAS 280, 1101
Phillips A., 2000, Geophys. Astrophys. Fluid Dyn., in press
Priklonsky V., Shukurov A., Sokoloff D., Soward A., 2000, Geophys. Astrophys. Fluid Dyn. (in press)
Pudritz R., 1981a, MNRAS 195, 881
Pudritz R., 1981b, MNRAS 195, 897
Regan M.W., Vogel S.N., Teuben P.J., 1997, ApJ 482, L143
Rüdiger G., Elstner D., Schultz M., 1993, A&A 270, 53
Ruzmaikin A., 1976, in: Stepanov V.E. (ed.), Plasma Astrophysics. Irkutsk
Ruzmaikin A.A., Shukurov A.M., Sokoloff D.D., 1988, Magnetic Fields of Galaxies. Dordrecht: Kluwer
Sakhibov F.Kh., Smirnov M.A., 1987, AZh 64, 255
Sakhibov F.Kh., Smirnov M.A., 1989, AZh 66, 921
Sakhibov F.Kh., Smirnov M.A., 1990, AZh 67, 690
Sanders D.B., Solomon P.M., Scoville N.Z., 1984, ApJ 276, 182
Shlosman I., Begelman M.C., Frank J., 1990, Nat 345, 679
Sofue Y., 1987, PASJ 39, 547
Stepinski T., Levy E.H., 1990, ApJ 362, 318
Subramanian K., Mestel L., 1993, MNRAS 265, 649